J|A|C|S COMMUNICATIONS

Published on Web 09/10/2010

Electric Field Destabilizes Noncovalent Protein−DNA Complexes

Michael U. Musheev, Yuri Filiptsev, Victor Okhonin, and Sergey N. Krylov*

Department of Chemistry and Centre for Research on Biomolecular Interactions, York University, Toronto, Ontario, M3J 1P3, Canada

Received June 30, 2010; E-mail: skrylov@yorku.ca

Abstract: Noncovalent protein−DNA interactions are involved in many vital biological processes. In cells, these interactions may take place in the environment of an electric field which originates from the plasma and organelle membranes and reaches strengths of 1 MV/cm. Moreover, protein−DNA interactions are often studied *in vitro* using an electric field as strong as 1 kV/cm, for example by electrophoresis. It is widely accepted that an electric field does not affect such interactions. Here we report on the first proof that an electric field of less than 1 kV/cm can destabilize the protein−DNA complexes through increasing the monomolecular rate constant of complex dissociation.

Noncovalent protein−DNA interactions are involved in many vital biological processes such as gene expression, DNA replication, DNA integrity control, DNA damage repair, and immune response.[1−3] In cells, such interactions may take place in the immediate proximity of the plasma and organelle membranes,[4,5] which generate a nonalternating electric field (simply electric field below) of up to 10^6 V/cm.[6,7] Moreover, protein−DNA interactions are often studied *in vitro* using an electric field as strong as 10^3 V/cm, for example by electrophoresis.[8,9] An electric field, thus, accompanies protein−DNA interactions in both nature and bioanalytical technologies; hence, it is important to understand how it can influence such interactions. Here we report on the first proof that an electric field can destabilize protein−DNA complexes through increasing the monomolecular rate constant, k_{off}, of complex dissociation. We showed at the quantitative level that other electric-field-associated phenomena, such as temperature increase, cannot account for the observed change in k_{off}, which reaches as much as 7-fold for an electric-field strength increasing from 0 to 600 V/cm. Our results suggest that the effect of an electric field on protein−DNA interactions must be taken into consideration while studying these interactions by electric-field-based techniques, such as electrophoresis. More intriguing, these results indicate that intracellular electric fields originating from mitochondrial membranes are certainly strong enough to affect protein−DNA interactions[6] and can, therefore, potentially contribute to the regulation of cellular processes.

To study the effect of the electric field on k_{off}, (i) the complex has to be placed in an electric field, (ii) free protein and DNA need to be continuously removed from the complex surroundings to allow for complex dissociation, and (iii) the kinetics of complex dissociation have to be followed. Interestingly, performing step one can facilitate steps two and three. There is a method, termed Non-Equilibrium Capillary Electrophoresis of Equilibrium Mixtures (NECEEM) that uses an electric field applied to capillary ends (step 1) to (i) continuously remove free protein and DNA from the complex (step 2) and (ii) record the kinetics of complex dissociation in a form of a NECEEM electropherogram (step 3) as schematically depicted in Figure 1A.[10] NECEEM was a method of choice in this work. Classical NECEEM utilizes a constant electric field and cannot measure k_{off} when the field strength is equal to zero. We developed "stopped-field" NECEEM to allow such measurements. In essence, stopped-field NECEEM starts with classical NECEEM, which is run for some time to separate the complex from free protein and DNA. The field is then stopped (turned off) for time τ, which is shorter than the equilibration time, to allow for complex dissociation without the field (see section 2 in the Supporting Information for more details on the equilibration time). Finally, the field is reintroduced to record the electropherogram. Complex dissociation during τ occurs without the electrophoretic displacement of protein and DNA and is manifested as a small peak on the exponential part of the NECEEM electropherogram (Figure 1B). Figure 1 illustrates how k_{off} with and without the electric field can be determined using simple algebraic formulas, which utilize only the values of four areas (A_1, A_2, $A_{1'}$, and $A_{2'}$) and one migration time (t_C) obtained directly from the electropherograms (see section 2 in the Supporting Information for derivations).

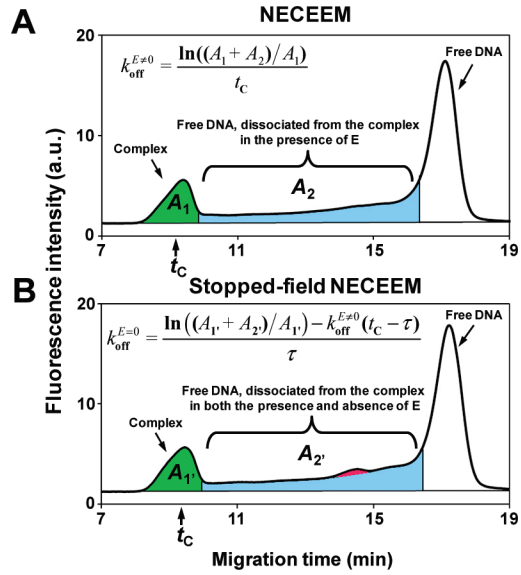

Figure 1. Electropherograms of classical NECEEM (A) and stopped-field NECEEM (B) for an equilibrium mixture of 100 nM MutS and 50 nM MutS aptamer, at 400 V/cm electric field. Classical NECEEM allows the determination of k_{off} in the presence of an electric field ($E = 0$) while stopped-field NECEEM facilitates the determination of k_{off} in the absence of an electric field ($E = 0$). A_1, A_2, $A_{1'}$, and $A_{2'}$ are the areas of corresponding colored features on the electropherograms, and τ is the time period during which $E = 0$. The red area represents the amount of DNA dissociated from the complex during the $E = 0$ period.

Using the method of k_{off} determination illustrated in Figure 1, we examined whether or not a detectable effect of the electric field on k_{off} can be observed. As our experimental model, we used a MutS protein and its DNA aptamer.[11] The experimental procedures

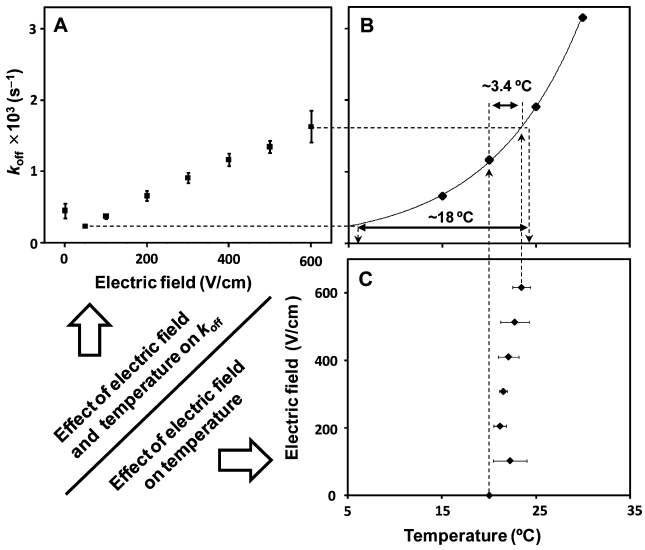

Figure 2. Effects of electric field and temperature on the rate constant of complex dissociation (k_{off}). (A) NECEEM-measured k_{off} values at different electric fields for the MutS-Aptamer complex. The zero-electric-field points were obtained by stopped-field NECEEM, while the nonzero-electric-field points were obtained using classical NECEEM. The experiments were performed at 20 °C. (B) NECEEM-measured k_{off} values for MutS-Aptamer complex at different temperatures and a constant electric field of 400 V/cm. (C) Temperature increase due to electric-field-associated Joule heating. The capillary coolant solution was thermostabilized at 20 °C. Temperature measurements were conducted using a diffusion-based method described elsewhere.[16] The electrophoresis buffer was 50 mM Tris-acetate pH 8.3.

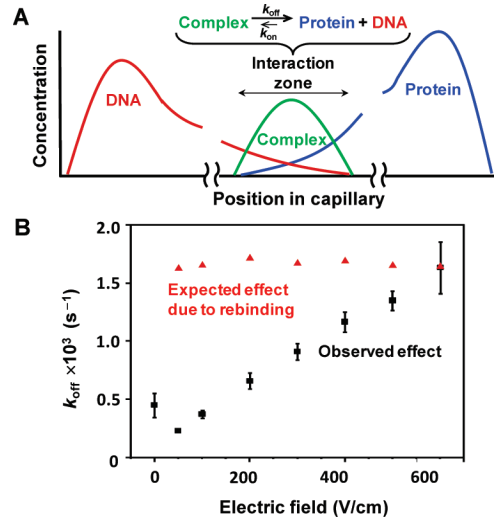

Figure 3. Effect of complex reassociation on k_{off} calculations in NECEEM. (A) Schematic showing the interaction zone where both dissociation and reassociation occur. The complex dissociates and releases protein and DNA, which move in opposite directions with respect to the complex. However, while still in the "interaction zone", the components have a chance to reassociate. (B) Illustration of the calculated maximum impact of complex reassociation on apparent k_{off} values (red triangles), which is negligible in comparison to the experimentally observed effect (black squares) (see section 4 of the Supporting Information for the method of calculations).

are detailed in section 1 of the Supporting Information. We found that k_{off} increased by about 7-fold when the electric field changed between 0 and 600 V/cm (Figure 2A; see also Figure S3 and Table S1 in the Supporting Information). Note that the differences between k_{off} values measured here and in the previous works are due to different run buffers used. Some evidence that an electric field may affect protein−DNA complex stability was previously reported by Kennedy and co-workers, but the influence was explained by "side effects" accompanying the electric field.[12] The first suggested side effect was a temperature increase inside the capillary due to Joule heat produced by an electric current. The rate constant of the complex dissociation increases with increasing temperature according to the Arrhenius equation. The second suggested side effect was rebinding of the protein and DNA dissociated from the protein−DNA complex in NECEEM before they are separated. The efficiency of this process is inversely related to the electric-field strength. In addition to the above-mentioned phenomena, we also need to consider processes at the capillary wall that were not previously suggested as potential side effects. One example of such a wall effect is mechanical stress, which may be experienced by the complex on the interface between the immobile and mobile ion layers, due to the high velocity gradient ranging from zero to the velocity of the electroosmotic flow.[13] The velocity of the electroosmotic flow increases with increasing electric field, which can potentially lead to increased tension and accelerated complex dissociation. There may be other wall effects, for example, a different pH near the walls,[14] which can also be confused with the electric-field effect if the wall effects are electric-field-dependent.

To demonstrate that an electric field itself can affect complex stability, we had to prove that the above side effects, even if present, could not quantitatively account for the experimentally observed increase in k_{off} with increasing electric-field strength.

The temperature inside the capillary inevitably grows with the electric-field strength;[15] the extent of this growth depends on the efficiency of heat dissipation from the capillary. Since k_{off} increases with increasing temperature, the temperature effect on k_{off} can potentially be confused with the effect of the electric field. To understand the extent to which temperature increase can affect k_{off}, we measured k_{off} values for a complex of MutS and its DNA aptamer at different temperatures (Figure 2B). We, then, measured the temperature in the capillary as a function of the electric field; a recently developed diffusion-based method was utilized (Figure 2C).[16] We found that the temperature inside the capillary grew by 3.4 ± 0.9 °C when the electric field increased from 0 to 600 V/cm. The observed temperature increase could only lead to a 1.3 times increase in k_{off} (see the lines projected from panel C to panel B) and, thus, could not account for the observed 7-fold increase in k_{off} when the field strength changed from 0 to 600 V/cm (Figure 2A). The data in Figure 2 show that the temperature needed to grow by more than 18 °C to fully account for the 7-fold increase in k_{off} (see the lines projected from panel A to panel B). We can, thus, conclude that temperature alone cannot explain complex destabilization with growing electric field.

DNA and protein dissociated from the complex can rebind again with a finite probability due to a finite length of the complex zone in NECEEM. This probability decreases with increasing electric-field strength as the electrophoretic velocities of the protein and DNA grow with the increasing strength. This, in turn, leads to the decrease of the reactants' residence time in the interaction zone (Figure 3A). The decreasing rate of field-dependent complex reassociation leads to an increase of the apparent k_{off} value. The decreasing rate of reassociation can, thus, be confused with a genuine electric-field-caused increase in k_{off}. We calculated the maximum potential impact of the reassociation process on the k_{off} value using experimentally determined velocities (of protein, DNA, and the complex), length of interaction zone, and time of interaction (Figure 3B). The decrease of the electric-field strength from 600 to 50 V/cm can only cause a 3% increase in the calculated k_{off}. This effect is smaller than the experimental error of k_{off} measurements and, thus, can be neglected. Therefore, we conclude that the combined effect of the temperature increase and complex reasso-

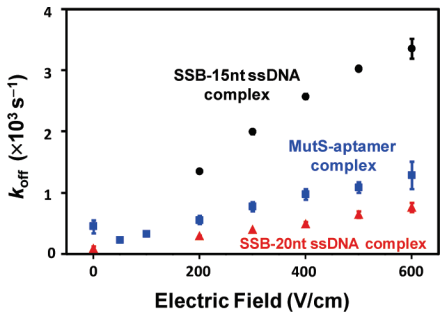

Figure 4. Effect of electric field on the rate of complex dissociation (k_{off}) for MutS with aptamer (blue squares), SSB with 15nt-ssDNA (black circles), and SSB with 20nt-ssDNA (red triangles). The effect of electric-field-associated temperature increase was subtracted using a procedure described in section 3 of the Supporting Information. For all experiments the capillary temperature was thermostabilized at 20 °C. Each point is represented by at least three different experiments, and an error is represented by 1 standard deviation.

ciation cannot account for the observed 7-fold increase in k_{off} with the field strength changing from 0 to 600 V/cm.

Finally, the rate of complex dissociation in the capillary volume may be different from the rate near the capillary walls due to various capillary-wall-associated effects (see above). To examine whether or not the wall effects can change k_{off}, we varied the capillary volume to surface ratio by changing its inner diameter. If the wall effects are measurable, a smaller-diameter capillary would have a higher k_{off} value. Experimentally, however, we observed that k_{off} dependence on the electric field was not distinguishable between capillaries with 50 and 75 μm inner diameters when the temperature effect was taken into account (see Figure S2 in section 3 of the Supporting Information). We can, thus, conclude that the combined influence of three side effects cannot account for the observed 7-fold increase in k_{off} with field strength increasing from 0 to 600 V/cm. Unless another unaccounted side effect exists, it is the electric field itself that destabilizes the protein−DNA complex.

To demonstrate that the observed electric-field effect on protein−DNA complex stability is not unique to the MutS-Aptamer complex, we also studied complexes of single-stranded DNA binding (SSB) protein with two different single-stranded (ss) DNA molecules (scrambled sequences of 20 and 15 nucleotides). The electric field accelerated the dissociation of the two SSB−DNA complexes, and the complex-destabilizing effect was different for all the studied protein−DNA pairs (Figure 4). We can, thus, conclude that the effect of the electric field on protein−DNA interactions depends on the interacting pair.

The mechanism for the effect of the electric-field strength on k_{off} is unknown; however it is quite logical to assume that due to the high negative charge of DNA, a protein−DNA complex is a strong dipole that tends to orient itself along an electric field. The electric field exerts an electrostatic force that pulls the protein and DNA away from each other. While this force may not be enough to break all the weak bonds at once, it can break a single bond without affecting others because of the flexibility of the DNA and protein. Other weak bonds can then be "opened" one-by-one like a "zipper". The suggested hypothetical mechanism is only one example of how an electric field can destabilize the complex.

Our finding has a number of important implications. First, a nonalternating and, likely, low-frequency alternating electric field can potentially affect cellular processes that involve protein−DNA complexes, e.g. gene expression, DNA replication, and DNA repair. Many other research groups reported different manifestations of the electric-field effect on cellular or animal models that can be potentially explained by the reported finding.[17−20] It is intriguing to learn whether or not endogenous electric fields, which always exist within cells, can regulate cellular processes and whether or not exogenous electric fields can inhibit these processes. Second, an electric field, which is routinely used in studies of protein−DNA interactions, can potentially lead to mistakes and misinterpretations. Electrophoresis is an example of a vulnerable technique, in particular, affinity capillary electrophoresis used for measuring equilibrium constants and NECEEM used for measuring k_{off}.[8,9] With the method developed in this work, one can study the effect of an electric field on specific protein−DNA interactions and take such effects into account.

To conclude, we outline our vision of future directions in this research area. It will be very interesting to experimentally test the ability of an electric field to affect the rate of formation of protein−DNA complexes (as opposed to the rate of complex dissociation studied in this work). Unfortunately, the method presented here is not suitable for such experiments. It is also very interesting to probe whether or not the electric field can inhibit the processes that rely on protein−DNA interactions *in vitro*. Examples of such processes include the polymerase chain reaction, *in vitro* transcription, restriction enzyme-catalyzed DNA digestion, and enzymatic DNA ligation. Progress in this area will also depend on the theoretical developments in the description of protein−DNA interactions and multibond affinity interactions in general. Finally, experiments must be designed to test the effect of an electric field on protein−DNA interactions in cells.

Acknowledgment. This work was funded by the Natural Sciences and Engineering Research Council of Canada. M.U.M. was supported by the Alexander Graham Bell Canada Graduate Scholarship, and Y.F. was supported by the Dr. James Wu Internship, York University.

Supporting Information Available: Supporting materials and methods and supporting results. This material is available free of charge via the Internet at http://pubs.acs.org.

References

(1) Ren, B.; Robert, F.; Wyrick, J. J.; Aparicio, O.; Jennings, E. G.; Simon, I.; Zeitlinger, J.; Schreiber, J.; Hannett, N.; Kanin, E.; Volkert, T. L.; Wilson, C. J.; Bell, S. P.; Young, R. A. *Science* **2000**, *290*, 2306–2309.
(2) Leng, F.; McMacken, R. *Proc. Natl. Acad. Sci. U.S.A.* **2002**, *99*, 9139–9144.
(3) Oh, D. B.; Kim, Y. G.; Rich, A. *Proc. Natl. Acad. Sci. U.S.A.* **2002**, *99*, 16666–16671.
(4) Jaffe, L. F. *Proc. Natl. Acad. Sci. U.S.A.* **1966**, *56*, 1102–1109.
(5) Siess, D. C.; Vedder, C. T.; Merksen, L. S.; Tanaka, T.; Freed, A. C.; McCoy, S. L.; Heinrich, M. C.; Deffebach, M. E.; Bennett, R. M.; Hefeneider, S. H. *J. Biol. Chem.* **2000**, *275*, 33655–33662.
(6) Tyner, K. M.; Kopelman, R.; Philbert, M. A. *Biophys. J.* **2007**, *93*, 1163–1174.
(7) Loew, L. M.; Tuft, R. A.; Carrington, W.; Fay, F. S. *Biophys. J.* **1993**, *65*, 2396–2407.
(8) Krylov, S. N. *Electrophoresis* **2007**, *28*, 69–88.
(9) Oestergaard, J.; Heegaard, N. H. H. *Electrophoresis* **2006**, *27*, 2590–2608.
(10) Berezovski, M.; Krylov, S. N. *J. Am. Chem. Soc.* **2002**, *124*, 13674–13675.
(11) Drabovich, A. P.; Berezovski, M.; Okhonin, V.; Krylov, S. N. *Anal. Chem.* **2006**, *78*, 3171–3178.
(12) Buchanan, D. D.; Jameson, E. E.; Perlette, J.; Malik, A.; Kennedy, R. T. *Electrophoresis* **2003**, *24*, 1375–1382.
(13) Jung, H.; Robison, A. D.; Cremer, P. S. *J. Am. Chem. Soc.* **2009**, *131*, 1006–1014.
(14) Tavares, M. F. M.; McGuffin, V. L. *Anal. Chem.* **1995**, *67*, 3687–3696.
(15) Evenhuis, C. J.; Haddad, P. R. *Electrophoresis* **2009**, *30*, 897–909.
(16) Musheev, M. U.; Javaherian, S.; Okhonin, V.; Krylov, S. N. *Anal. Chem.* **2008**, *80*, 6752–6727.
(17) Luther, K. C. *Int. J. Low. Extrem. Wounds* **2005**, *4*, 23–44.
(18) Okudan, B.; Keskin, A. U.; Aydin, M. A.; Cesur, G.; Comlekci, S.; Suslu, H. *Bioelectromagnetics* **2006**, *27*, 589–592.
(19) Vernier, P. T.; Sun, Y.; Marcu, L.; Salemi, S.; Craft, C. M.; Gundersen, M. A. *Biochem. Biophys. Res. Commun.* **2003**, *310*, 286–295.
(20) Reynaud, J. A.; Labbe, H.; Lequoc, K.; Lequoc, D.; Nicolau, C. *FEBS Lett.* **1989**, *247*, 106–112.

JA105754H

SUPPORTING INFORMATION

Electric Field Destabilizes Non-Covalent Protein-DNA Complexes

Michael U. Musheev, Yuri Filiptsev, Victor Okhonin, Sergey N. Krylov *

Department of Chemistry and Centre for Research on Biomolecular Interactions, York University, Toronto, Ontario, M3J 1P3, Canada

Table of Contents

1. Supporting Materials and Methods

Materials. Recombinant MutS and SSB proteins both from *E. coli* were purchased from Sigma-Aldrich (Oakville, ON, Canada). The HPLC purified, fluorescently labeled MutS aptamer (5'-fluorescein-CTT CTG CCC GCC TCC TTC CTC GGG GTT AGA ACG TCG TGT AGG ACT CCT ATC GGT TTA TGG AGA CGA GAT AGG CGG ACA CT), and 15-nucleotide scrambled single stranded DNA (5'-Fluorescein-GCG GAG CGT GGC AGG) were purchased from IDT DNA Technology Inc. (Coralville, IA, USA) and dissolved in a TE buffer (10 mM Tris-HCl, 0.1 mM EDTA, pH 7.5) to have a 100 μM stock solution and be stored at -20 °C. All other chemicals were purchased from Sigma-Aldrich (Oakville, ON, Canada). Uncoated fused-silica capillaries with 75 or 50 μm inner diameter (375 μm outer diameter) were purchased from Polymicro (Phoenix, AZ, USA). The capillary was mounted on a capillary electrophoresis (CE) instrument (P/ACE MDQ, Beckman Coulter, Fullerton, CA, USA), which was equipped with temperature-controlled sample storage and thermal control of the capillary. All solutions were made using deionized water filtered through a 0.22 μm filter (Millipore, Nepean, ON, Canada).

Methods. The MutS aptamer was first prepared at a concentration of 1 μM in a MutS sample buffer (50 mM Tris-Acetate pH 8.3 supplemented with 2.5 mM $MgCl_2$), and "annealed" by heating to 80 °C for 3 min and cooling down to 20 °C at a rate of 7.5 °C/min. The "annealed" aptamer and MutS were mixed in the MutS sample buffer to their final concentration of 50 and 100 nM, respectively. The mixture was incubated at 4 °C for 5 hours to allow for equilibrium to establish. The equilibrium mixture was divided in two parts and each part was placed in a separate Beckman CE-MDQ instrument. One instrument was used to perform NECEEM experiments with varying electric fields. The second instrument was used to repeatedly perform identical NECEEM experiment with constant electric field strength of 400 V/cm. NECEEM electropherograms from the second instrument were compared with each other to confirm that they were identical. This ensured that the "equilibrium mixture" was at equilibrium and all its components retained their concentrations and activities constant over the duration of all experiments. NECEEM measures equilibrium constants K_d (or K_b) based on the concentrations of the free molecules and the complexes in the equilibrium mixture before NECEEM separation. In the other words, NECEEM has a memory of equilibrium; therefore, the measurements of equilibrium constants by NECEEM are not affected by the electric field. We used the constancy of K_d as an additional indicator of the stability of our experimental system. In this work, the values of equilibrium dissociation constant, K_d, were equal within the limit of experimental error for all NECEEM experiments (see **Table S1** below). Approximately 30 nL of the equilibrium mixture was injected into a capillary by a pressure pulse of 0.5 psi for 5 s and moved along the first 5 cm of capillary length by the second pressure pulse of 1 psi for 30 s to reach a thermo-stabilized region of the capillary. An electric field was then applied to facilitate electrophoretic separation. The electrophoresis buffer in all MutS experiments was 50 mM Tris-Acetate pH 8.3 supplemented with 2.5 mM $MgCl_2$. An equilibrium mixture of 200 nM SSB and 100 nM DNA was prepared and treated in a similar manner except for using a different incubation/electrophoresis buffer: 50 mM Tris-Acetate at pH 8.3 with no $MgCl_2$ added. Every experimental point in a graph of k_{off} versus the electric field strength is an average of 3 to 10 experiments performed over a period of several months confirming the reproducibility of results. The order of experiments with different electric field strengths was shuffled to avoid any potential reagent-stability-related artifacts.

2. Determination of k_{off} at zero strength of electric field

In the following derivations, to distinguish between amounts and concentrations, we use figure and square brackets, respectively. The stopped-field NECEEM approach includes four major steps. First, the equilibrium mixture of protein and DNA with an initial amount of the protein-DNA complex equal

to $\{C\}_0$ is injected into a capillary. Second, an electric field is applied to the capillary to separate the components of the equilibrium mixture. During this step, the complex is dissociating in the presence of the electric field and after time t_1 the amount of the remaining complex, $\{C\}_1$, equals to:

$$\{C\}_1 = \{C\}_0 \times e^{-k_{off}^{E\neq 0} \times t_1} \quad \textbf{S1}$$

In the third step, the electric field is turned off and the complex present in amount $\{C\}_1$ is allowed to dissociate during time τ in the absence of electric field. The required condition during step 3 for the calculation is that the rate of complex dissociation is greater than that of complex re-association:

$$k_{on}^{E=0} \times [P^*] \times [DNA^*] << k_{off}^{E=0} [C]_1 \quad \textbf{S2}$$

[DNA*] and [P*] are concentrations of free DNA and protein which formed by complex dissociation during time τ. The above requirement is crucial since it assures that the impact of the re-association process, during this zero-field step, on the dissociation process is negligible. In this case the re-association process can only introduce an insignificant systematic error by underestimating the actual k_{off} value for the zero electric-field strength. The values of k_{on} under the zero-electric field conditions were obtained as described in the end of this section (equations S8, S9). The amount of complex remaining intact at the end of step 3, $\{C\}_2$, is:

$$\{C\}_2 = \{C\}_1 \times e^{-k_{off}^{E=0} \times \tau} \quad \textbf{S3}$$

Finally, during the 4th step, which lasts for time t_2, an electric field is reapplied and the amount of complex which reaches the detector equals to:

$$\{C\} = \{C\}_2 \times e^{-k_{off}^{E\neq 0} \times t_2} \quad \textbf{S4}$$

Finally combining equations S1, S3, and S4 we obtain the amount of complex which reached the detector:

$$\{C\} = \{C\}_0 \times e^{-(k_{off}^{E\neq 0} \times (t_2 + t_1) + k_{off}^{E=0} \times \tau)} \quad \textbf{S5}$$

Rearranging equation S5 for k_{off} unaffected by an electric field we get:

$$k_{off}^{E=0} = \frac{\ln(\{C\}_0 / \{C\}) - k_{off}^{E\neq 0}(t_1 + t_2)}{\tau} \quad \textbf{S6}$$

The sum of times t_1, t_2, and τ is equal to the time complex traveled from the start of the separation to the detection or in the other words, the migration time of the complex (t_c in **Fig. 2B**). $\{C\}_0 / \{C\}_1$ is equal to the ratio of areas $(A_{1'} + A_{2'})/A_{1'}$ (**Fig. 1** in the main text) and equation S6 can be rewritten as :

$$k_{off}^{E=0} = \frac{\ln((A_{1'} + A_{2'})/A_{1'}) - k_{off}^{E\neq 0}(t_C - \tau)}{\tau} \quad \textbf{S7}$$

To obtain k_{on} values at zero-electric field for equations S2-S3 above we used the following equation:

$$k_{on} = \frac{k_{off}}{K_d} \quad \textbf{S8}$$

where K_d is an equilibrium dissociation constant, which can be obtained from the areas on a NECEEM electropherogram and total initial concentrations of DNA and protein; $[DNA]_0$ and $[P]_0$, respectively:

$$K_d = \frac{[P]_0(1+R) - [DNA]_0}{1 + 1/R}; \quad R = \frac{[DNA]_{eq}}{[C]_{eq}} = \frac{A_3}{A_2 + A_1} \quad \textbf{S9}$$

where A_1, A_2, and A_3 are the areas illustrated in **Fig. 1A** in main text. Subscript "eq" indicates equilibrium concentrations. The derivation of expression S9 can be found in *Analyst* **2003**, *128*, 571-575.

The K_d value was calculated for a system at equilibrium before the application of an electric field. The value of k_{on} at a zero electric field was calculated using equation S8, above mentioned K_d value and a k_{off} value measured at the lowest electric field of 50 V/cm, assuming that the zero-electric field k_{off} value would be close to the 50 V/cm value. This assumption is acceptable because the obtained values were only used to validate condition S2.

3. Measurement and subtraction of temperature effect on k_{off}

The actual temperature inside the capillary at different electric fields was measured by a previously described diffusion-based method (*Anal. Chem.* **2008**, *80*, 6752-6757) (**Fig. S1A**). To subtract the temperature effect from the cumulative effect of electric field on the data in **Fig. 2A** of the main text we first measured the k_{off} values for MutS-aptamer complex at different temperatures (**Fig. 2B** in main text). We then adjusted the temperature values according to **Fig. 2C** in main text, to account for the temperature increase due to Joule heating (**Fig. S1B)**. Finally, by using the dotted lines in the two graphs of **Fig. S1,** we calculated the influence of Joule-heating-associated temperature effect on k_{off} at different electric field strengths.

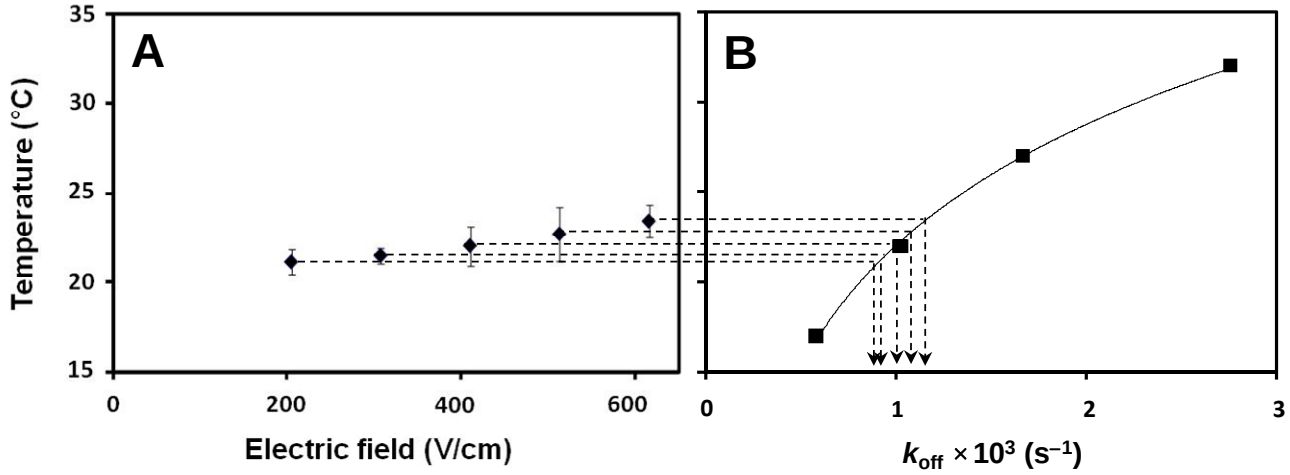

Figure S1. Effect of temperature on k_{off} for MutS-aptamer complex. Panel **A** shows temperature increase due to electric-field-associated Joule heating. The capillary coolant solution was thermo-stabilized at 20 °C. Temperature measurements were conducted using a diffusion-based method with fluorescein as a diffusion probe. The running buffer was 50 mM Tris-acetate at pH 8.3. Panel **B** illustrates effect of temperature on k_{off}. The NECCEM experiments for k_{off} measurements were performed at 400 V/cm. The running buffer was 50 mM Tris-acetate at pH 8.3 supplemented with 2.5 mM $MgCl_2$. The capillary in all experiments had an inner diameter of 75 μm.

4. Determination of effect of complex re-association during NECEEM measurements on k_{off}

Equations which approximately describe the behavior of the protein and DNA formed by complex dissociation in NECEEM separation are:

$$\frac{\partial[\mathrm{P}]}{\partial t}+(v_{\mathrm{P}}-v_{\mathrm{C}})\frac{\partial[\mathrm{P}]}{\partial x}=k_{\mathrm{off}}[\mathrm{C}](x)\,\mathrm{e}^{-k_{\mathrm{off}}t} \qquad \textbf{S10}$$

$$\frac{\partial[\mathrm{DNA}]}{\partial t}+(v_{\mathrm{DNA}}-v_{\mathrm{C}})\frac{\partial[\mathrm{DNA}]}{\partial x}=k_{\mathrm{off}}[\mathrm{C}](x)\,\mathrm{e}^{-k_{\mathrm{off}}t}$$

where v_{C}, v_{P}, v_{DNA}, [C], [P] and [DNA] are the velocities and concentrations of the complex, free protein, and free DNA, respectively, k_{off} is a dissociation rate constant, and x is the distance from the middle of a complex plug. In these equations, it is assumed that the complex, which reforms from the previously dissociated protein and DNA, does not dissociate the second time. Next, assuming that $v_{\mathrm{P}} > v_{\mathrm{C}} > v_{\mathrm{DNA}}$, $[\mathrm{P}] = 0$ for $x = +\infty$, and $[\mathrm{DNA}] = 0$ for $x = +\infty$, we get the following solution for equations S10:

$$[\mathrm{P}]=\frac{k_{\mathrm{off}}}{v_{\mathrm{P}}-v_{\mathrm{C}}}e^{(-k_{\mathrm{off}}t)}\int_0^{\infty}[\mathrm{C}](x+y)e^{\left(\frac{-k_{\mathrm{off}}}{v_{\mathrm{P}}-v_{\mathrm{C}}}y\right)}dy \qquad \textbf{S11}$$

$$[\mathrm{DNA}]=\frac{k_{\mathrm{off}}}{v_{\mathrm{C}}-v_{\mathrm{DNA}}}e^{(-k_{\mathrm{off}}t)}\int_0^{\infty}[\mathrm{C}](x-y)e^{\left(\frac{-k_{\mathrm{off}}}{v_{\mathrm{C}}-v_{\mathrm{DNA}}}y\right)}dy$$

The re- association process occurs only in a short spatial region with a length equal to the length of the injected plug. In a situation when $\left(v_{\mathrm{P}}-v_{\mathrm{C}}\right)/k_{\mathrm{off}}$ and $\left(v_{\mathrm{C}}-v_{\mathrm{DNA}}\right)/k_{\mathrm{off}}$ are much greater than the length of the injected plug, equation S11 can be written as:

$$[\mathrm{P}]\approx\frac{k_{\mathrm{off}}}{v_{\mathrm{P}}-v_{\mathrm{C}}}e^{(-k_{\mathrm{off}}t)}\int_0^{\infty}[\mathrm{C}](x+y)dy \qquad \textbf{S12}$$

$$[\mathrm{DNA}]\approx\frac{k_{\mathrm{off}}}{v_{\mathrm{C}}-v_{\mathrm{DNA}}}e^{(-k_{\mathrm{off}}t)}\int_0^{\infty}[\mathrm{C}](x-y)dy$$

Using equations S12, the rate of complex re-association from previously dissociated protein and DNA, is described by the following approximate expression:

$$k_{\mathrm{on}}[\mathrm{P}](x,t)[\mathrm{DNA}](x,t)\approx\frac{k_{\mathrm{off}}^2e^{(-2k_{\mathrm{off}}t)}}{(v_{\mathrm{P}}-v_{\mathrm{C}})(v_{\mathrm{C}}-v_{\mathrm{DNA}})}\int_0^{\infty}[\mathrm{C}](x+y)dy\int_0^{\infty}[\mathrm{C}](x-y)dy \qquad \textbf{S13}$$

This expression can be calculated for the case of the Gaussian shape of spatial concentration distribution within a plug of complex, having a width at a height of 1/*e* equal to *L:*

$$[\mathrm{C}](x')=[\mathrm{C}]_0e^{(-(2x'/L)^2)} \qquad \textbf{S14}$$

In particular, for the highest concentration of C, at the center of the Gaussian peak (at $x = 0$) described by equation S14, expression S13 transforms into:

$$k_{\mathrm{on}}[\mathrm{P}](0,t)[\mathrm{DNA}](0,t)\approx\frac{\pi k_{\mathrm{on}}L^2k_{\mathrm{off}}^2e^{(-2k_{\mathrm{off}}t)}}{16(v_{\mathrm{P}}-v_{\mathrm{C}})(v_{\mathrm{C}}-v_{\mathrm{DNA}})}[\mathrm{C}]_0^2 \qquad \textbf{S15}$$

Alternatively to S14, the rate of complex dissociation at the center of the Gaussian peak can be described by the following expression:

$$k_{\text{off}}[\text{C}](0,t) = k_{\text{off}}[\text{C}]_0 e^{(-k_{\text{off}}t)} \quad \textbf{S16}$$

Then, by combining equations S15 and S16 we can find the ratio between the rates of re-association and dissociation:

$$\frac{k_{\text{on}}[\text{P}](0,t)[\text{DNA}](0,t)}{k_{\text{off}}[\text{C}](0,t)} = \frac{C_0 \pi k_{\text{on}} L^2 k_{\text{off}} e^{(-k_{\text{off}}t)}}{16(v_{\text{P}} - v_{\text{C}})(v_{\text{C}} - v_{\text{DNA}})} \quad \textbf{S17}$$

Finally, equation S17, allows one to predict the effect of re-association on calculated values of k_{off} from NECEEM electropherograms. The dissociation rate constant affected by the re-association process (k'_{off}) is equal to:

$$k'_{\text{off}} = k_{\text{off}} \left(1 - \frac{C_0 \pi k_{\text{on}} L^2 k_{\text{off}} e^{(-k_{\text{off}}t)}}{16(v_{\text{P}} - v_{\text{C}})(v_{\text{C}} - v_{\text{DNA}})} \right) \quad \textbf{S18}$$

To calculate the impact of complex reformation we used a k_{off} value determined from a NECEEM experiment conducted at the highest electric field strength (E = 600 V/cm), when the re-association process has smallest effect on the accuracy of measured k_{off}. By using this experimental k_{off} as a reference point and by using experimentally measured v_{C}, v_{P}, and v_{DNA} we calculated values of k'_{off} at different electric field strengths (**Fig. 3B,** red triangles) and validated the assumption that complex re-association had no effect on k_{off} determination from NECEEM experiments conducted in a range of studied electric field strengths (50-600 V/cm).

5. Additional Information

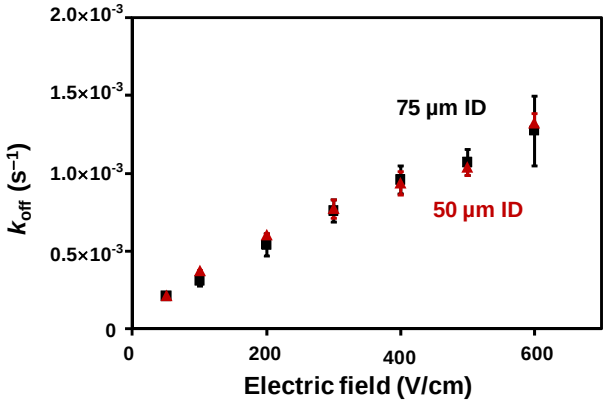

Figure S2. Effect of capillary diameter on k_{off} for MutS-aptamer complex. The capillary coolant solution was thermo-stabilized at 20 °C. NECCEM experiments for k_{off} measurements were performed in capillaries with inner diameters of 50 µm (red triangles) and 75 µm (black squares). The effect of electric field-associated temperature increase was subtracted using a procedure described in section 3. The electrophoresis buffer was 50 mM Tris-acetate pH 8.3 supplemented with 2.5 mM $MgCl_2$.

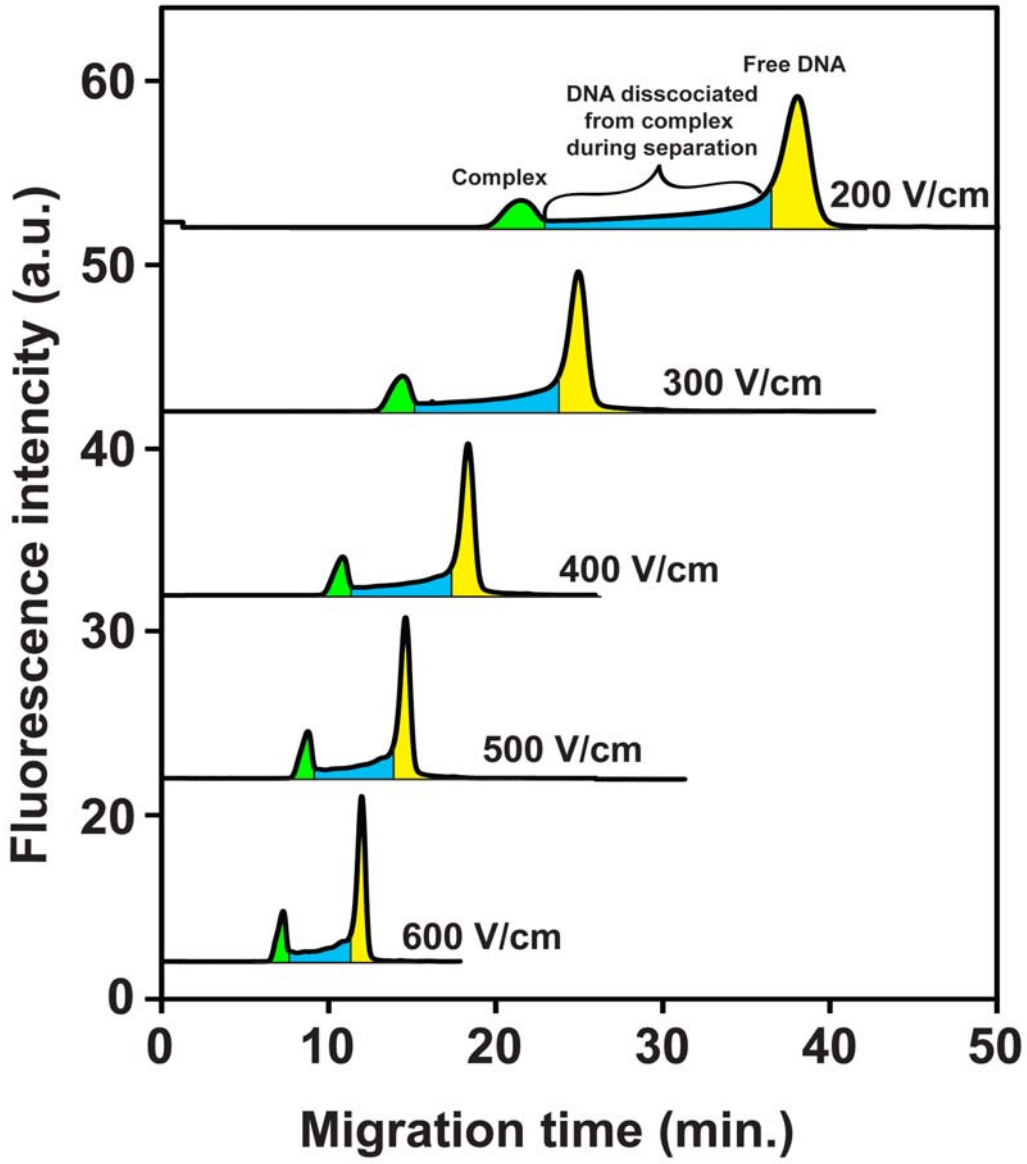

Figure S3. NECEEM electropherograms of MutS and its DNA aptamer obtained at different electric-field strengths. The equilibrium mixture contained 50 nM aptamer and 100 nM MutS in 50 mM Tris-acetate buffer (pH 8.3) supplemented with 2.5 mM $MgCl_2$. The fused silica capillary with 75-μm inner diameter was used. The capillary coolant solution was thermo-stabilized at 20 °C. The boundaries between the blue and yellow areas were found by superimposing the yellow peak with a peak of DNA obtained from a run of DNA only. The areas of the features in each electropherogram and the calculated vales of k_{off} and K_d are shown in **Table S1**.

Table S1. NEEEM-based determination of K_d and k_{off} at different electric field strengths. The areas listed in columns 1-3 correspond to peaks of free DNA, intact complex reaching the detector, and DNA dissociated from the complex during separation (see **Fig. S3**). Columns 4-6 contain to the normalized areas. The areas from column 1 and 3 were divided by the migration time of free DNA (with subtracted time of pressure-driven propagation, 1 min). The areas from column 2 were divided by the migration time of the complex (with subtracted time of pressure-driven propagation, 1 min). The k_{off} values were then determined by using the normalized areas and the equation presented in **Fig. 1A** in the main text. The K_d values were calculated using the normalized areas and the total concentrations of the protein and DNA (100 and 50 nM, respectively) in the equilibrium mixture; the approach was described in detail in reference 9 in the main text.

Area of free DNA	Area of complex	Area of DNA dissociated from complex	Normalized area of free DNA	Normalized area of complex	Normalized area of dissociated DNA	K_d (nM)	k_{off} (s^{-1})	Electric field (V/cm)
3.36	1.01	1.48	0.305	0.295	0.134	77.9	1.61×10^{-3}	600
4.06	1.18	1.89	0.299	0.291	0.139	77.3	1.39×10^{-3}	500
2.10	0.54	0.97	0.119	0.109	0.055	82.7	1.18×10^{-3}	400
6.29	1.61	3.25	0.266	0.259	0.138	77.6	0.95×10^{-3}	300
8.77	1.88	4.96	0.245	0.233	0.139	79.7	0.75×10^{-3}	200